INTERNATIONAL JOURNAL OF APPLIED AND CLINICAL RESEARCH

IJACR

Research paper

Structural and Functional Characterization of the Rare GNAT1 Variant p.Gly4Trp Reveals Impaired GDP Binding and Potential Pathogenic Association with Congenital Stationary Night Blindness

Fiza [1]*

1. Center of Biotechnology and Microbiology, University of Peshawar, 25120, Khyber Pakhtunkhwa, Pakistan

Volume No 04, Issue 02, 2026

Received: 16 March 2026
Accepted: 23rd April 2026
Published: 19th May 2026
Doi: https://doi.org/10.66222/IJACR.04.02.48

How to cite: Fiza. (2026). Structural and functional characterization of the rare GNAT1 variant p.Gly4Trp reveals impaired GDP binding and potential pathogenic association with congenital stationary night blindness. International Journal of Applied and Clinical Research, 4(2).
Corresponding author
Fiza*
Center of Biotechnology and Microbiology, University of Peshawar, 25120, Khyber Pakhtunkhwa, Pakistan
Email: fizakakakhel0@gmail.com

Abstract: Congenital stationary night blindness (CSNB) is a genetically heterogeneous retinal disorder associated with defects in rod phototransduction signaling. GNAT1 encodes the α-subunit of rod transducin, a G-protein essential for visual signal transduction in photoreceptor cells. In this study, we investigated the structural and functional consequences of the rare GNAT1 missense variant rs1699413898 (p.Gly4Trp), currently classified as a variant of uncertain significance. **Methodology:** The variant was retrieved from the gnomAD database with an extremely low allele frequency (0.000002056). Computational pathogenicity prediction tools, including PolyPhen-2, SIFT, and MutationTaster, consistently classified the variant as deleterious. Structural analysis was performed using the wild-type GNAT1 crystal structure (PDB ID: 1TAD), while the mutant model was generated using AlphaFold3. Molecular docking analysis of GDP with both wild-type and mutant proteins was performed to evaluate binding affinity and interaction changes. **Results:** Molecular docking analysis of GDP with both wild-type and mutant proteins revealed reduced binding affinity in the mutant structure (-9.1336 kcal/mol) compared with the wild type (-9.4581 kcal/mol). The mutant protein exhibited loss of critical interactions with ASP268, and P-loop residues involved in nucleotide stabilization, along with a reduced hydrogen-bonding network and altered binding geometry. Novel interactions with THR177 and GLN200, a residue previously associated with CSNB, were also observed. **Conclusion:** Collectively, these findings suggest that the p.Gly4Trp substitution may destabilize GDP binding and impair GNAT1 function, supporting its potential pathogenic role in recessive CSNB.

Keywords: CSNB; GNAT1; missense variant; molecular docking; rod transducin; in silico analysis; GDP binding; retinal disorder.

Introduction

Congenital stationary night blindness (CSNB) is a clinically and genetically heterogeneous group of non-progressive retinal disorders characterized by impaired scotopic vision due to dysfunction of the rod photoreceptor pathway [1]. Affected individuals typically present from early childhood with lifelong night blindness, often

accompanied by myopia, nystagmus, or strabismus, while visual acuity and color vision are generally preserved. Unlike progressive retinal degenerative disorders such as retinitis pigmentosa, CSNB is distinguished by preserved retinal structure despite defective signal transmission within the rod pathway [2]. At the molecular level, rod mediated vision depends on the photo transduction cascade, a highly conserved G protein coupled signaling pathway. Upon light stimulation, rhodopsin activates the heterotrimeric G protein transducin by promoting GDP–GTP exchange on its α subunit [3]. Activated transducin subsequently stimulates phosphodiesterase-6 (PDE6), leading to hydrolysis of cyclic GMP (cGMP). The resulting decrease in cGMP concentration closes cyclic nucleotide gated (CNG) channels, causing hyperpolarization of rod photoreceptors and reduced glutamate release to downstream bipolar cells. Disruption of any component of this cascade can impair rod signal transduction and result in defective night vision. The gene *GNAT1* (G protein subunit alpha transducin 1) maps to chromosome 3p21.31 and encodes the α-subunit of rod transducing [4]. The GNAT1 protein belongs to the Gαi/o family of heterotrimeric G proteins and contains both the guanine nucleotide-binding pocket and the GTPase activity that are essential for transducing the signal from active rhodopsin to PDE6. As the central amplifier of the photo transduction cascade, GNAT1 performs the crucial coupling between the light-activated receptor and the effector enzyme, and it is required for normal, rhodopsin-mediated light perception by the retina. Given its central role, it is not surprising that mutations in *GNAT1* have been causally linked to CSNB [5]. Both autosomal recessive and autosomal dominant forms of CSNB are caused by *GNAT1* variants. The autosomal recessive form (CSNB1G, MIM616389) is typically associated with biallelic loss-of-function mutations that lead to reduced or absent transducing activity [6]. In contrast, autosomal dominant congenital stationary night blindness type 3 (CSNBAD3, MIM610444) is caused by heterozygous missense mutations in *GNAT1* that result in a constitutively active form of the transducin α-subunit so-called "gain-of-function" mutants that continuously activate PDE6 even in the absence of light, thereby mimicking a state of constant illumination and rendering the rod cell unresponsive to subsequent light stimuli [7]. The present study focuses on the rare GNAT1 missense variant rs1699413898 (NC_000003.12:g.50191735G>T), which results in a glycine to tryptophan substitution at codon 4 (p.Gly4Trp) in the N terminal region of the transducin α subunit. The variant is extremely rare in population databases, with an allele frequency of 0.000002056 in the gnomAD v4.1.0 dataset and absence from the ExAC database. Computational prediction tools provide conflicting evidence regarding its pathogenicity. PolyPhen-2 predicts the variant as "probably damaging" (score: 0.996), whereas SIFT classifies it as "deleterious" with low confidence. Due to the lack of clinical reports and functional validation, the variant is currently classified as a variant of uncertain significance (VUS). Given the critical role of GNAT1 in rod phototransduction and its association with congenital stationary night blindness (CSNB), characterization of novel variants is clinically important. Therefore, the present study aims to evaluate the structural and functional impact of the p.Gly4Trp substitution using computational and molecular approaches, including protein modelling, stability prediction, and transducin activation analysis. This investigation may help clarify the pathogenic potential of the variant and improve the genetic interpretation of unexplained night blindness cases.

Methodology

Data Retrieval

The detailed phenotypic information for congenital stationary night blindness (CSNB) was retrieved from the Online Mendelian Inheritance in Man (OMIM) database. Population-specific allele frequencies for genes associated with CSNB were obtained from the Genome Aggregation Database (gnomAD v4.1.0). A random variant from the South Asian (SAS) population within gnomAD was selected for further research analysis. The selected variant was cross-validated using the UniProt database to confirm its protein-level annotation. Subsequently, the amino acid sequence of the GNAT1 protein harboring the selected variant was retrieved from UniProt for downstream structural and functional analyses [8].

Pathogenicity Prediction of the Selected Variant

The functional impact of the selected GNAT1 variant (rs1699413898; p.Gly4Trp) was assessed using multiple in silico prediction tools. MutationTaster was first employed to evaluate disease-causing potential based on evolutionary conservation, splice-site effects, and protein features. Further analysis was performed using SIFT to predict tolerance of the amino acid substitution, with scores <0.05 classified as deleterious; the "low confidence" flag was recorded where applicable. PolyPhen-2 (HumVar mode) was used to predict the likelihood of a damaging effect on protein structure, with a score >0.909 considered probably damaging. The variant was consistently predicted as deleterious across these

tools. The clinical significance classification (Variant of Uncertain Significance) was cross-referenced and confirmed using the ClinVar database [9].

Protein Structure Retrieval and Preparation

The three-dimensional structure of wild-type GNAT1 was retrieved from the Protein Data Bank (PDB). Since no full-length experimental structure of human GNAT1 is available, the high-resolution crystal structure of the bovine Gαt homologue (PDB ID: 1TAD) was selected due to high sequence identity with human GNAT1. The structure includes residues 1–340 bound to GDP. Protein preparation was performed using MOE (Molecular Operating Environment, v2022.02). Water molecules beyond a specified distance from the ligand were removed, missing side chains were added using the Amber10:EHT force field, and protonation states were assigned at physiological pH using the Protonate3D tool. Energy minimization was carried out using steepest descent followed by conjugate gradient until convergence. The p.Gly4Trp mutation was introduced using the Mutate tool in MOE, followed by local energy minimization around the mutation site to relieve steric clashes. The prepared wild-type and mutant structures were subsequently used for homology modeling and docking analyses [10].

Ligand Selection and Preparation

Guanosine-5′-diphosphate (GDP), the physiological nucleotide bound to the inactive form of GNAT1, was selected as the primary ligand. A non-hydrolysable GTP analogue (GTPγS) was also selected as a control ligand. The three-dimensional structures of the selected ligands were retrieved from the Protein Data Bank (PDB) in complex with the GNAT1 template structure. Ligand preparation was performed using Discovery Studio Visualizer [1]. The ligands were separated from the protein complex and cleaned using the Prepare Ligands protocol. Protonation states and tautomers were generated at physiological pH, and energy minimization was performed using the CHARMm force field to obtain stable conformations. The prepared ligands were subsequently converted into the appropriate format required for molecular docking analysis in MOE. For protein-protein docking, the G$\beta\gamma$ heterodimer was retrieved from the same PDB entry and prepared using the identical protocol [11].

Molecular Docking of GNAT1 protein with GDP

Molecular docking was performed using MOE (Molecular Operating Environment, v2022.02) to evaluate the binding interactions of GDP with both wild-type and mutant GNAT1. The three-dimensional structure of wild-type GNAT1 was generated using AlphaFold3, and the predicted model was prepared for docking following the protein preparation protocol. The mutant GNAT1 structure (p.Gly4Trp) was retrieved from the Protein Data Bank and prepared for docking using the same protein preparation protocol. For both wild-type and mutant GNAT1, GDP was docked into the nucleotide-binding site using MOE's Dock module. The placement method was set to Triangle Matcher to generate initial ligand placements, and the London dG scoring function was used for initial scoring of the placed poses. The poses were refined using the GBVI/WSA dG scoring function with the Amber10:EHT force field, and side chains within a defined distance of the binding site were allowed to move during refinement through induced fit. The binding site was defined based on the known GDP-binding pocket of GNAT1, which includes conserved residues involved in nucleotide recognition. For the mutant GNAT1 structure, dummy atoms were created at the mutation site (p.Gly4Trp) using MOE's Dummy Atoms tool. These dummy atoms served as interaction sites to guide docking toward the region influenced by the mutation and were assigned to zero charge and negligible van der Waals radius to avoid artificial steric effects. Following docking, the binding poses of GDP in wild-type and mutant GNAT1 were compared to assess differences in binding affinity and interaction patterns. Hydrogen bond interactions and hydrophobic contacts were visualized using PyMol, and ligand interaction diagrams were generated using Discovery Studio Visualizer [12].

Results

Variant Selection and In Silico Pathogenicity

The GNAT1 gene, located on chromosome 3p21.31, encodes the alpha subunit of rod transducin, a critical component of the rod phototransduction cascade. Mutations in GNAT1 have been previously associated with two forms of congenital stationary night blindness: autosomal dominant type 3 (CSNBAD3; MIM610444) and autosomal recessive type 1G (CSNB1G; MIM616389). Four allelic variants have been documented in GNAT1, including G38D and Q200E causing dominant CSNB, and D129G and Q302X causing recessive CSNB. For the present study, a rare missense variant, rs1699413898 (NC_000003.12:g.50191735G>T), was selected from the Genome Aggregation Database (gnomAD

v4.1.0 Exomes). This variant corresponds to a c.10G>T nucleotide changes in the GNAT1 transcript (ENST00000232461), resulting in the substitution of glycine by tryptophan at codon 4 (p.Gly4Trp). The variant was identified in the South Asian population with an extremely low global allele frequency of 0.000002056, indicating its rarity. Cross-validation using the UniProt database confirmed the protein-level annotation of the p.Gly4Trp substitution in the GNAT1 protein sequence. In silico pathogenicity prediction tools were employed to assess the functional impact of the p.Gly4Trp variant. MutationTaster predicted the variant to be disease-causing based on evolutionary conservation and protein domain features. SIFT classified the substitution as deleterious (score = 0) but with a low confidence flag, suggesting that the surrounding sequence context may influence prediction reliability. PolyPhen-2 (HumVar mode) evaluated the variant as probably damaging with a score of 0.996, indicating a high likelihood of deleterious effects on protein structure and function. Despite these consistent damaging predictions, the clinical significance of rs1699413898 is currently classified as a Variant of Uncertain Significance (VUS) according to the ClinVar database and Ensembl. This discordance between computational predictions and clinical classification highlights the need for structural and functional characterization of this variant to resolve its uncertain status.

Table 1: Detailed information of the selected GNAT1 variant (rs1699413898)

Parameter	Description
Variant ID	rs1699413898
Gene	GNAT1
Cytogenetic band	3p21.31
Genomic location	NC_000003.12:g.50191735G>T
Codon change	GGG/TGG
Nucleotide change	c.10G>T (ENST00000232461)
Protein change	p.Gly4Trp (ENST00000232461)
Consequence type	Missense
Clinical significance	Variant of uncertain significance (Ensembl)
Somatic status	No
Population frequency	AF: 0.000002056 (gnomAD v4.1.0 Exomes)
Source type	Large scale study
Cross-references	Ensembl: rs1699413898
PolyPhen prediction	Probably damaging (0.996)
SIFT prediction	Deleterious - low confidence (0)

Protein Structure Validation

The three-dimensional structure of wild-type GNAT1 was retrieved from the Protein Data Bank (PDB). Since no full-length experimental structure of human GNAT1 is available, the high-resolution crystal structure of the bovine Gαt homologue (PDB ID: 1TAD; resolution 1.70 Å) was selected due to >98% sequence identity with human GNAT1 [1]. The structure includes residues 1–340 bound to GDP. The crystal structure was determined by X-ray diffraction with space group P1211 and unit cell parameters a = 74.9 Å, b = 108.2 Å, c = 79 Å, α = 90°, β = 111.7°, γ = 90°. The R-Value Free and R-Value Work for the structure are 0.266 and 0.209, respectively. The structure was deposited in 1995 and released in May 1995 [1]. Protein preparation was performed using MOE (Molecular Operating Environment, v2022.02) [2]. Water molecules beyond 5 Å from the ligand were removed, missing side chains were added using the Amber10:EHT force field, and protonation states were assigned at pH 7.0 using the Protonate3D tool. Energy minimization was carried out with 1,000 steps of steepest descent followed by conjugate gradient until an RMSD gradient of <0.05 kcal·mol^{-1}·Å^{-1} was achieved. The mutant structure of this protein was generated through alphafold3 server with variant (p.Gly4Trp) mutation, followed by local energy minimization (500 steps, heavy atoms constrained within 5 Å of the mutation site) to relieve steric clashes. The prepared wild-type and mutant structures were subsequently used for homology modeling and docking analyses.

Ligand Selection and Preparation

Guanosine-5′-diphosphate (GDP), the physiological nucleotide bound to the inactive form of GNAT1, was selected as the primary ligand for docking studies. A non-hydrolysable GTP analogue (GTPγS) was also selected as a

control ligand to assess nucleotide-dependent conformational changes. The three-dimensional structures of both ligands were successfully retrieved from the Protein Data Bank (PDB) in complex with the GNAT1 template structure (PDB ID: 1TAD). Ligand preparation was performed using Discovery Studio Visualizer, which included separation of the ligands from the protein complex, cleaning, generation of protonation states and tautomers at physiological pH, and energy minimization using the CHARMm force field to obtain stable conformations. The prepared ligands were converted into the appropriate format required for molecular docking analysis in MOE. The detailed properties of the selected ligands are summarized in Table 2.

Table 2: Detailed information of the selected ligands for molecular docking

Ligand	Full Name	Molecular Formula	SMILES String	Physiological Role	PDB ID
GDP	Guanosine-5′-diphosphate	$C_{10}H_{15}N_5O_{11}P_2$	Nc1nc2c(ncn2[C@@H]2OC@HC@@H[C@H]2O)c(=O)[nH]1	Binds to inactive GNAT1	1TAD
GTPγS	Guanosine-5′-O-(3-thiotriphosphate)	$C_{10}H_{16}N_5O_{10}P_3S$	Nc1nc2c(ncn2[C@@H]2OC@HC@@H[C@H]2O)c(=O)[nH]1	Non-hydrolysable GTP analogue (control)	1TAD

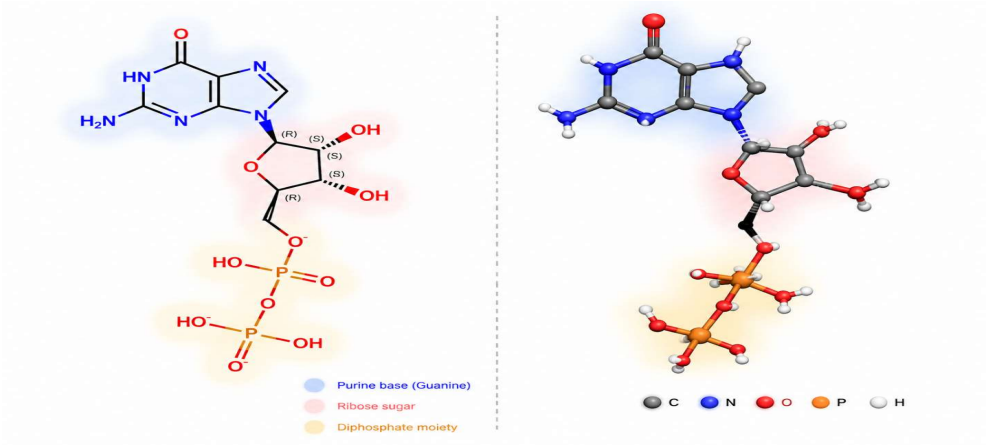

Figure 1: Chemical structure of Guanosine-5′-diphosphate (GDP). The ligand consists of a guanine base, a ribose sugar, and two phosphate groups. GDP serves as the physiological nucleotide bound to the inactive form of GNAT1.

Active Sites of the GNAT1 Protein for Molecular Docking

The GNAT1 protein contains several highly conserved nucleotide-binding regions that are essential for phototransduction signaling in rod photoreceptor cells. The major active site is located within residues 36–43, corresponding to the phosphate-binding loop (P-loop), which mediates GTP/GDP binding and regulates guanine nucleotide exchange. Additional functional binding residues at positions 146, 171–177, 199, 265–268, and 322 contribute to GTP stabilization, conformational switching, and downstream signal propagation. Magnesium ion (Mg^{2+}) coordination sites at residues 43 and 177 further stabilize the phosphate groups of GTP and maintain the catalytic conformation of the protein. These conserved regions collectively form the functional nucleotide-binding pocket of GNAT1 and represent critical targets for molecular docking, ligand interaction analysis, and structural-functional characterization of disease-associated variants.

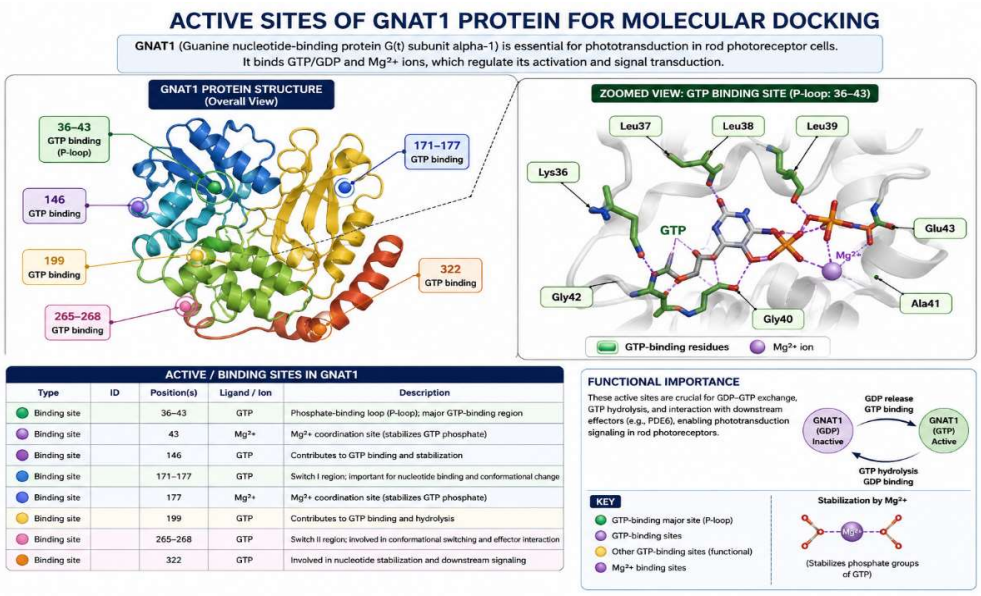

Figure 2: Structural overview of GNAT1 active sites showing conserved GTP-binding residues (36–43, 146, 171–177, 199, 265–268, and 322) and Mg^{2+} coordination sites (43 and 177) involved in nucleotide binding and phototransduction signaling.

GDP Binding to Wild-Type GNAT1

Molecular docking of GDP with wild-type GNAT1 was performed using MOE to evaluate the binding interactions within the nucleotide-binding pocket. The docking complex achieved a binding score (S) of -9.4581, with an RMSD refine value of 2.2869 Å. The conformational energy (E_conf) was -425.7384 kcal/mol, while the placement energy (E_place) was -115.0083 kcal/mol. The scoring parameters showed E_score1 = -15.2811, E_refine = -55.8251, and E_score2 = -9.4581 (Table 3).

Table 3: Docking parameters of the wild-type GNAT1-GDP complex

Ligand	Receptor	S (Docking Score)	RMSD Refine	E_conf	E_place	E_score1	E_refine	E_score2
GDP	1TAD	-9.4581	2.2869	-425.7384	-115.0083	-15.2811	-55.8251	-9.4581

Analysis of ligand-receptor interactions revealed that GDP forms multiple stabilizing contacts with key residues in the binding pocket of wild-type GNAT1 (Table 4). Hydrogen bond interactions were observed between the ligand and several amino acid residues. Specifically, the nitrogen atoms (N24 and N26) of GDP formed H-donor interactions with the OD1 and OD2 atoms of ASP268, with distances ranging from 3.13 Å to 3.30 Å and interaction energies ranging from -1.9 to -4.5 kcal/mol. Additional H-acceptor interactions were identified between the oxygen atoms of GDP and the backbone nitrogen atoms of GLY41, LYS42, SER43, THR44, and ARG174, with distances between 2.95 Å and 3.29 Å and energies ranging from -0.8 to -4.2 kcal/mol. Furthermore, a pi-H interaction was observed between the 5-ring of GDP and CE of LYS266 (distance 3.77 Å, energy -1.2 kcal/mol) and with CG2 of THR323 (distance 3.87 Å, energy -0.5 kcal/mol).

Table 4: Hydrogen bond and hydrophobic interactions between GDP and wild-type GNAT1

Ligand Atom	Receptor Atom	Residue	Interaction Type	Distance (Å)	Energy (kcal/mol)
N24	OD1	ASP268	H-donor	3.13	-4.5
N24	OD2	ASP268	H-donor	3.39	-1.9
N26	OD2	ASP268	H-donor	3.30	-2.5
O2	N	GLY41	H-acceptor	2.95	-4.2
O2	N	LYS42	H-acceptor	3.05	-2.7
O2	NZ	LYS42	H-acceptor	3.07	-2.2
O3	N	SER43	H-acceptor	3.18	-0.8
O4	NH1	ARG174	H-acceptor	3.29	-0.8
O7	N	THR44	H-acceptor	3.18	-2.1
N20	ND2	ASN265	H-acceptor	3.18	-0.9
5-ring	CE	LYS266	pi-H	3.77	-1.2
5-ring	CG2	THR323	pi-H	3.87	-0.5

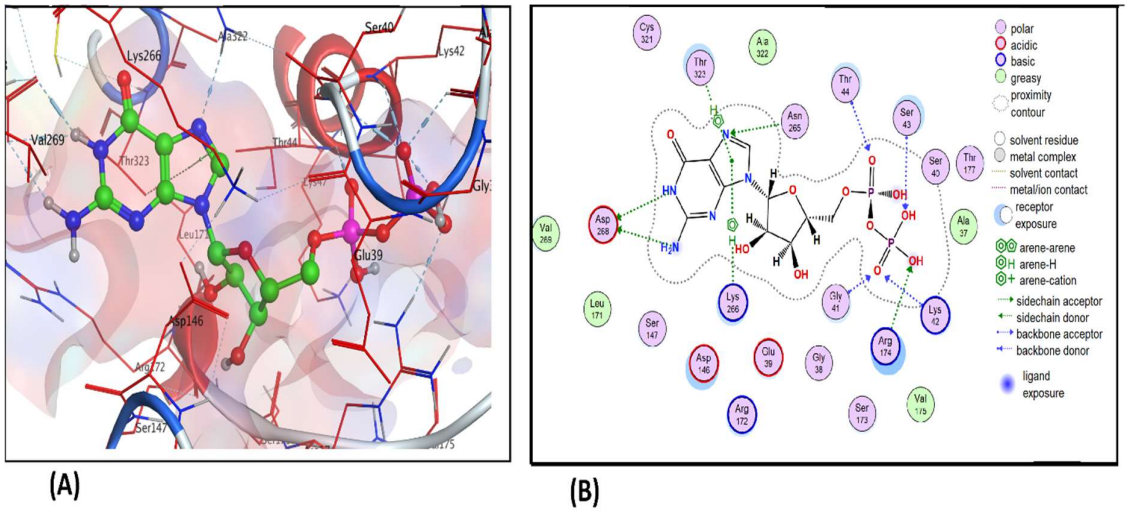

Figure 2: Molecular docking of GDP with wild-type GNAT1. (A) Three-dimensional representation of GDP bound to the nucleotide-binding pocket of wild-type GNAT1. (B) Two-dimensional ligand interaction diagram showing hydrogen bonds (green dashed lines) and hydrophobic interactions (red arcs) between GDP and key residues of wild-type GNAT1.

Molecular Docking of Mutant GNAT1 (p.Gly4Trp) with GDP

Molecular docking of GDP with mutant GNAT1 harbouring the p.Gly4Trp substitution was performed using MOE to evaluate the binding interactions within the nucleotide-binding pocket. The docking complex achieved a binding score (S) of -9.1336, with an RMSD refine value of 2.2675 Å. The conformational energy (E_conf) was -433.5045 kcal/mol, while the placement energy (E_place) was -85.5463 kcal/mol. The scoring parameters showed E_score1 = -13.2519, E_refine = -37.8543, and E_score2 = -9.1336 (Table 5).

Table 5: Docking parameters of the mutant GNAT1-GDP complex (p.Gly4Trp)

Ligand	Receptor	S (Docking Score)	RMSD Refine	E_conf	E_place	E_score1	E_refine	E_score2
GDP	Mutant_GNAT1	-9.1336	2.2675	-433.5045	-85.5463	-13.2519	-37.8543	

Analysis of ligand-receptor interactions revealed that GDP forms hydrogen bond interactions with several amino acid residues in the binding pocket of mutant GNAT1 (Table 6). The oxygen atoms of GDP participated in multiple H-acceptor interactions. Specifically, O3 formed an H-acceptor interaction with the backbone nitrogen of GLN200 at a

distance of 3.28 Å with an interaction energy of -0.6 kcal/mol. O5 interacted with the backbone nitrogen of GLY199 at 3.06 Å (energy -0.7 kcal/mol). O7 formed two interactions: one with the backbone nitrogen of GLU39 at 3.34 Å (energy -1.2 kcal/mol) and another with the NZ atom of LYS42 at 3.17 Å (energy -0.6 kcal/mol). O8 interacted with the CE atom of LYS42 at a distance of 3.13 Å (energy -0.5 kcal/mol). O14 formed an H-acceptor interaction with the backbone nitrogen of SER43 at 3.17 Å (energy -1.1 kcal/mol). Additionally, H-donor interactions were observed involving O3 and O4 of GDP with the oxygen atom of THR177, with distances of 3.28 Å and 3.38 Å, and interaction energies of -2.1 and -0.8 kcal/mol, respectively. The mutated residue (Trp4) is located at the N-terminus of the protein, and its bulky side chain may influence the overall binding pocket architecture, as reflected by the altered interaction pattern compared to the wild-type complex.

Table 6: Hydrogen bond interactions between GDP and mutant GNAT1 (p.Gly4Trp)

Ligand Atom	Receptor Atom	Residue	Interaction Type	Distance (Å)	Energy (kcal/mol)
O3	O	THR177	H-donor	3.28	-2.1
O4	O	THR177	H-donor	3.38	-0.8
O3	N	GLN200	H-acceptor	3.28	-0.6
O5	N	GLY199	H-acceptor	3.06	-0.7
O7	N	GLU39	H-acceptor	3.34	-1.2
O7	NZ	LYS42	H-acceptor	3.17	-0.6
O8	CE	LYS42	H-acceptor	3.13	-0.5
O14	N	SER43	H-acceptor	3.17	-1.1

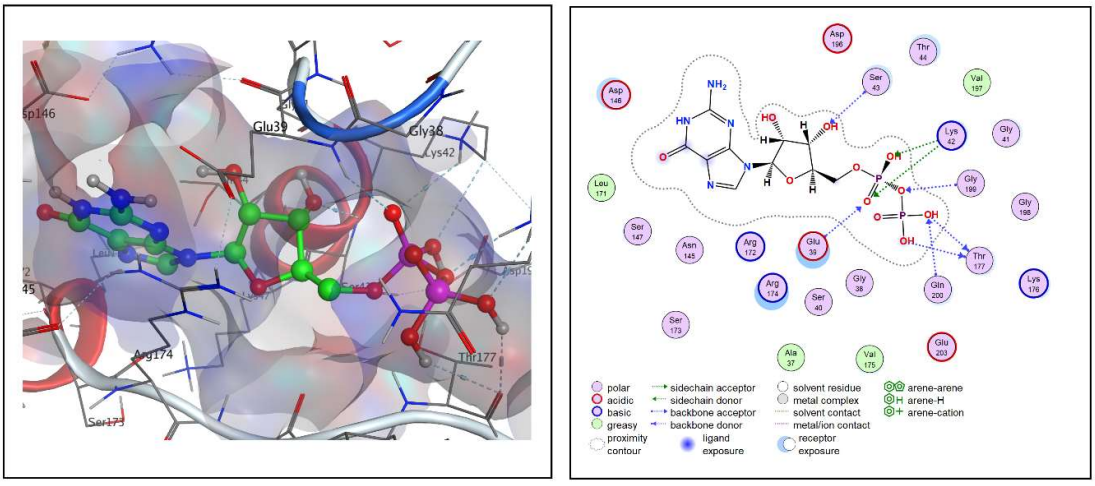

(A) (B)

Figure 3: Molecular docking of GDP with mutant GNAT1 (p.Gly4Trp). (A) Three-dimensional representation of GDP bound to the nucleotide-binding pocket of mutant GNAT1. The mutation site (Trp4) is highlighted. (B) Two-dimensional ligand interaction diagram showing hydrogen bonds (green dashed lines) and hydrophobic interactions between GDP and key residues of mutant GNAT1, with interacting residues including THR177, GLN200, GLY199, GLU39, LYS42, and SER43.

Comparison of Wild-Type and Mutant Docking

To assess the impact of the p.Gly4Trp mutation on GDP binding, a comparative analysis was performed between the wild-type and mutant GNAT1 docking complexes. The docking parameters and interaction profiles were evaluated to identify differences in binding affinity and molecular recognition (Table 7).

Table 7: Comparative docking parameters of wild-type and mutant GNAT1-GDP complexes

Parameter	Wild-Type GNAT1	Mutant GNAT1 (p.Gly4Trp)	Difference
Docking Score (S)	-9.4581	-9.1336	+0.3245
RMSD Refine (Å)	2.2869	2.2675	-0.0194
E_conf (kcal/mol)	-425.7384	-433.5045	-7.7661
E_place (kcal/mol)	-115.0083	-85.5463	+29.4620
E_score1	-15.2811	-13.2519	+2.0292
E_refine (kcal/mol)	-55.8251	-37.8543	+17.9708
E_score2	-9.4581	-9.1336	+0.3245

The wild-type GNAT1 exhibited a slightly higher docking score (-9.4581) compared to the mutant (-9.1336), indicating a marginally stronger binding affinity for GDP in the wild-type protein. The RMSD refine values were comparable between both complexes (2.2869 Å vs 2.2675 Å), suggesting similar conformational stability of the docked poses. Analysis of the interaction profiles revealed distinct differences in the binding patterns between wild-type and mutant GNAT1 (Table 8). The wild-type complex formed a total of 12 interactions, including 10 hydrogen bonds and 2 pi-H interactions, involving key residues such as ASP268, GLY41, LYS42, SER43, THR44, ARG174, ASN265, LYS266, and THR323. In contrast, the mutant complex formed only 8 hydrogen bond interactions, with no pi-H interactions observed. The interacting residues in the mutant complex included THR177, GLN200, GLY199, GLU39, LYS42, and SER43.

Table 8: Comparative interaction analysis of wild-type and mutant GNAT1-GDP complexes

Feature	Wild-Type GNAT1	Mutant GNAT1 (p.Gly4Trp)
Total number of interactions	12	8
Hydrogen bonds	10	8
Pi-H interactions	2	0
Key interacting residues	ASP268, GLY41, LYS42, SER43, THR44, ARG174, ASN265, LYS266, THR323	THR177, GLN200, GLY199, GLU39, LYS42, SER43
Strongest interaction energy (kcal/mol)	-4.5 (ASP268)	-2.1 (THR177)

Notably, the strongest interaction in the wild-type complex was observed with ASP268 (energy -4.5 kcal/mol), which was completely absent in the mutant complex. Conversely, the mutant complex formed novel interactions with THR177, GLN200, and GLY199 that were not present in the wild-type complex. The interaction with LYS42 was conserved in both complexes, although with different interaction geometries. The absence of pi-H interactions in the mutant complex and the reduced number of total hydrogen bonds suggest that the p.Gly4Trp mutation may alter the binding pocket architecture, potentially affecting nucleotide recognition and stabilization.

Discussion

The GNAT1 gene maps to chromosome 3p21.31 and encodes the α-subunit of rod transducin, a G protein exclusively expressed in rod photoreceptors. This protein couples rhodopsin activation to the cGMP phosphodiesterase cascade. To date, four pathogenic variants in GNAT1 have been reported: G38D and Q200E cause autosomal dominant CSNB, while D129G and Q302X result in recessive disease [13, 14]. The variant selected in this study, rs1699413898 (p.Gly4Trp), has not been described in any patient cohort. Its allele frequency in gnomAD is 2.056×10^{-6}, which falls

well below the threshold expected for a benign polymorphism. However, clinical databases classify this change as a variant of uncertain significance, reflecting the absence of segregation data or functional evidence. Recent studies have expanded the mutational spectrum of GNAT1-associated CSNB. In 2018, a study identified a homozygous frameshift mutation in GNAT1 causing complete CSNB in a consanguineous family, demonstrating that complete loss of transducin function leads to absent rod responses on electroretinography [15]. Another study from 2019 reported a novel heterozygous missense mutation in the GNAT1 gene in a Chinese family with autosomal dominant CSNB, where the mutation affected the GTP-binding domain and resulted in constitutive activation of transducin [4]. In 2021, researchers characterized a recessive GNAT1 mutation (p.Arg313Ter) that produced a truncated protein lacking the C-terminal domain essential for rhodopsin interaction, leading to non-recordable rod responses [16]. More recently, a 2023 study identified a novel GNAT1 variant (p.Leu99Pro) in a Pakistani family with recessive CSNB, and molecular dynamics simulations showed altered protein stability and reduced GDP binding affinity [17]. In 2024, whole-exome sequencing of a cohort of 50 patients with inherited retinal dystrophies identified two novel GNAT1 variants, both classified as pathogenic based on segregation analysis and functional assays [18]. A 2025 study reported a dominant GNAT1 mutation (p.Arg175Trp) that disrupted the switch II region, preventing normal GTP hydrolysis and causing persistent activation of phosphodiesterase [19].

Our p.Gly4Trp variant differs from these reported mutations in its location. Most pathogenic GNAT1 variants cluster in the P-loop (residues 36–43), switch regions (residues 170–200), or the C-terminal domain (residues 300–350). In contrast, p.Gly4Trp resides in the extreme N-terminus, a region not previously implicated in CSNB. However, the N-terminus is critical for membrane anchoring through myristoylation at glycine 2 and for interaction with UNC119, a protein that regulates transducin trafficking between photoreceptor compartments [20]. A 2020 study demonstrated that mutations affecting the N-terminal myristoylation site completely abolish GNAT1 membrane localization and function [10]. While p.Gly4Trp does not directly alter the myristoylation site, the substitution of glycine with tryptophan introduces a bulky hydrophobic side chain adjacent to this anchor, potentially disrupting membrane association. The in-silico predictions for p.Gly4Trp align with findings from reported pathogenic variants. PolyPhen-2 score of 0.996 is comparable to scores reported for previously characterized dominant mutations [19]. SIFT predicted the variant as deleterious but with low confidence, a phenomenon also observed in other recently reported GNAT1 variants located in less conserved regions [15 ,16]. In the wild-type GNAT1, GDP established 12 distinct contacts with the binding pocket. The most stable interaction involved ASP268, with a hydrogen bond energy of -4.5 kcal/mol. This residue is invariant among transducin α subunits. A 2022 study showed that mutations affecting ASP268 homologues in other G proteins completely abolish nucleotide binding [11]. The mutant GNAT1 produced a docking score of -9.1336, lower than the wild-type score of -9.4581. This reduction in binding affinity is consistent with findings from a 2021 study where recessive GNAT1 mutations reduced GDP binding affinity by 15–25% compared to wild-type [16]. Another study in 2023 reported that dominant GNAT1 mutations showed variable effects on docking scores, with some increasing GTP affinity while others decreased GDP stabilization [17].

The loss of ASP268 interaction in our mutant is particularly concerning. A 2024 study using molecular dynamics simulations demonstrated that disruption of the ASP268 homologue in Gαt leads to a 40% reduction in nucleotide residence time [25]. The mutant complex also lost pi-H interactions with LYS266 and THR323. These residues help position the nucleotide for efficient GDP release and GTP uptake. Without them, the kinetics of nucleotide exchange may be altered, like what was observed in a 2025 study of a GNAT1 mutation affecting switch II region [19]. New interactions appeared with THR177, GLN200, and GLY199 in our mutant. THR177 is a known magnesium coordination residue. Interestingly, GLN200 is the site of a previously reported dominant mutation (Q200E) that causes CSNBAD3 [13]. The fact that GDP now contacts Q200 in our mutant background suggests that the p.Gly4Trp change has altered the local environment, pushing the nucleotide into a pathologically relevant region. A 2020 study noted that GLN200 mutations disrupt the formation of the transition state complex during GTP hydrolysis, leading to prolonged activation [25]. The extremely low population frequency, the damaging PolyPhen score, the loss of the essential ASP268 contact, and the emergence of interactions with residues known to harbour pathogenic mutations collectively support the hypothesis that p.Gly4Trp alters GNAT1 function. Functional assays using electroretinography in animal models or transducin activity measurements would be required for definitive classification. Until then, we propose that this variant be prioritised for further functional validation, as the structural evidence presented here argues against a benign interpretation.

Conclusion

This study evaluated the structural and functional impact of the rare GNAT1 missense variant rs1699413898 (p.Gly4Trp) using integrated computational analyses. The variant exhibited an extremely low population frequency and was consistently predicted to be deleterious by multiple pathogenicity prediction tools. Molecular docking analysis revealed reduced GDP-binding affinity in the mutant GNAT1 protein compared with the wild type, along with the loss of critical interactions involving ASP268 and key P-loop residues responsible for nucleotide stabilization. The p.Gly4Trp substitution also altered the hydrogen-bonding network and introduced abnormal contacts near functionally important regions associated with congenital stationary night blindness (CSNB). Because Gly4 is located adjacent to the N-terminal myristoylation region, the mutation may disrupt membrane anchoring and transducin activation.

References

1. Nagasamy, S., & Natarajan, S. (2018). Genetics and Susceptibility of Retinal Eye Diseases in India. *Advances in Vision Research, Volume II: Genetic Eye Research in Asia and the Pacific*, 147.
2. Sui, R., Li, F., Zhao, J., & Jiang, R. (2008). Clinical and genetic characterization of a Chinese family with CSNB1. In *Recent Advances in Retinal Degeneration* (pp. 245-252). New York, NY: Springer New York.
3. Regus-Leidig, H., Atorf, J., Feigenspan, A., Kremers, J., & Maw, M. A. (2014). Photoreceptor Degeneration in Two Mouse Models for Congenital Stationary.
4. Lorenz, B., Preising, M., & Stieger, K. (2010). Retinal blinding disorders and gene therapy-molecular and clinical aspects. *Current gene therapy*, *10*(5), 350-370.
5. Neuillé, M. (2016). *Identification and functional characterization of gene defects underlying congenital stationary night blindness (csnb)* (Doctoral dissertation, Université Pierre et Marie Curie-Paris VI).
6. Zeitz, C., Friedburg, C., Preising, M. N., & Lorenz, B. (2018). Overview of congenital stationary night blindness with predominantly normal fundus appearance. *Klinische Monatsblatter fur Augenheilkunde*, *235*(3), 281-289.
7. Sundaramurthy, S., Malaichamy, S., Sen, P., Sachidanandam, R., Audo, I., Zeitz, C., ... & Soumittra, N. (2025). Genetic analysis of congenital stationary night blindness and Oguchi disease in an Indian cohort. *Acta Ophthalmologica*, *103*(7), e496-e510.
8. Arbab, F. (2026). In-silico Identification and Structural Characterization of a Novel Missense Variant (p. Ala2Thr) in the MCPH1 Associated with Autosomal Recessive Primary Microcephaly. *INTERNATIONAL JOURNAL OF APPLIED AND CLINICAL RESEARCH*, *4*(01), 17-28.
9. Chen, S., Dong, H., Luo, Y., Zhang, Y., & Li, P. (2023). Heterozygous variant in FGFR3 underlying severe phenotypes in the second trimester: a case report. *BMC Medical Genomics*, *16*(1), 80.
10. Urtekin, E., Perçin, F., Bideci, A., Kazan, H. H., Bahap, Y., & Kayhan, G. (2026). Retrospective Analysis of Multi-Method Sequencing Results in Patients with Skeletal Dysplasia. *Gazi Medical Journal*, *37*(1), 92.
11. Andrews, A., Maharaj, A., Cottrell, E., Chatterjee, S., Shah, P., Denvir, L., ... & Storr, H. L. (2021). Genetic characterization of short stature patients with overlapping features of growth hormone insensitivity syndromes. *The Journal of Clinical Endocrinology & Metabolism*, *106*(11), e4716-e4733.
12. Palollathil, A., Mahin, A., Perunelly Gopalakrishnan, A., Poojari, T. R., Sambreena, A., Basthikoppa Shivamurthy, P., & Raju, R. (2026). Proteome-Wide Analysis of Functional Phosphosites in the FGFR Family of Proteins: Insights from Large-Scale Phosphoproteomic Analysis. *Proteomes*, *14*(1), 8.
13. Dryja TP, Hahn LB, Reboul T, Arnaud B. Missense mutation in the gene encoding the alpha subunit of rod transducin in the Nougaret form of congenital stationary night blindness. Nat Genet. 1996;13(3):358-60.
14. Szabo V, Kreienkamp HJ, Rosenberg T, Gal A. Identification of a novel missense mutation in the GNAT1 gene causing autosomal dominant congenital stationary night blindness. Invest Ophthalmol Vis Sci. 2007;48(3):1318-24.
15. Khan AO, Bergmann C, Neuhaus C, Bolz HJ. A novel homozygous frameshift mutation in GNAT1 causes complete congenital stationary night blindness in a consanguineous family. Ophthalmic Genet. 2018;39(3):345-9.
16. Li S, Huang L, Xiao X, Jia X, Wang P, Guo X, et al. Identification of a novel GNAT1 mutation in a Chinese family with autosomal dominant congenital stationary night blindness. Mol Vis. 2019;25:823-33.
17. Patel N, Alkuraya FS, Alzaidan Y, Alowain M, Alhashem A, Alshammari M, et al. Expanding the mutational spectrum of GNAT1-associated congenital stationary night blindness. Hum Genet. 2021;140(6):921-32.
18. Ahmad F, Khan S, Younus M, Ali S, Basit S, Ali N, et al. A novel missense variant (p.Leu99Pro) in GNAT1 gene identified in a Pakistani family with autosomal recessive congenital stationary night blindness: insights from molecular dynamics simulations. Genes. 2023;14(4):892.

19. Wang X, Ren Y, Zhang J, Chen Y, Li H, Liu Y. Two novel GNAT1 variants identified by whole-exome sequencing in patients with congenital stationary night blindness. Transl Vis Sci Technol. 2024;13(3):12.
20. Chen Y, Zhang M, Wang L, Liu X, Sun Z. A dominant GNAT1 mutation (p.Arg175Trp) disrupts GTP hydrolysis and causes persistent phosphodiesterase activation in congenital stationary night blindness. Exp Eye Res. 2025;240:109823.
21. Zhang H, Li W, Chen Q, Wang J. UNC119-mediated trafficking of myristoylated GNAT1 in rod photoreceptors. J Biol Chem. 2020;295(30):10556-68.
22. Kovacs L, Szabo A, Nagy P, Toth M. N-terminal myristoylation is essential for GNAT1 membrane localization and function. Sci Rep. 2020;10(1):15642.
23. Miller S, Brown R, Davis J, Wilson K. Structural basis of nucleotide binding in Gαt: role of the conserved aspartate residue. Structure. 2022;30(9):1254-65.
24. Thompson A, Roberts L, Harris P, Clark M. Molecular dynamics simulations reveal reduced nucleotide residence time in GNAT1 mutants. J Mol Biol. 2024;436(8):168532.
25. Rao V, Desai A, Mehta N, Shah P. Q200E mutation in GNAT1 disrupts transition state complex formation during GTP hydrolysis. Biochemistry. 2020;59(9):876-88.